Bandwidth Analysis of Multiport Radio-Frequency Systems—Part I

Ding Nie, *Student Member, IEEE,* and Bertrand M. Hochwald, *Fellow, IEEE*

***Abstract*—When multiple radio-frequency sources are connected to multiple loads through a passive multiport matching network, perfect power transfer to the loads across all frequencies is generally impossible. In this two-part paper, we provide analyses of bandwidth over which power transfer is possible. Our principal tools include broadband multiport matching upper bounds, presented herein, on the integral over all frequency of the logarithm of a suitably defined power loss ratio. In general, the larger the integral, the larger the bandwidth over which power transfer can be accomplished. We apply these bounds in several ways: We show how the number of sources and loads, and the coupling between loads, affect achievable bandwidth. We analyze the bandwidth of networks constrained to have certain architectures. We characterize systems whose bandwidths scale as the ratio between the numbers of loads and sources.**

The first part of the paper presents the bounds and uses them to analyze loads whose frequency responses can be represented by analytical circuit models. The second part analyzes the bandwidth of realistic loads whose frequency responses are available numerically. We provide applications to wireless transmitters where the loads are antennas being driven by amplifiers. The derivations of the bounds are also included.

***Index Terms*—Bandwidth, Bode-Fano bounds, broadband matching bounds, non-reciprocal networks, passive matching networks, radio-frequency coupling**

I. Introduction

Analyses of the bandwidth over which power can be transferred in radio-frequency (RF) systems are often limited to a single source and load because of the complexity in manipulating multiport matching networks and multiple loads. Factors that contribute to the complexity include defining appropriate measures of bandwidth when there are many sources and loads, and the difficulty of analyzing coupling between loads. We propose methods of analysis that utilize broadband performance bounds applicable to a wide class of passive networks and an arbitrary number of sources and dissipative loads.

The ability to transfer power from sources to loads relies, in part, on the ability to match the impedance of the sources to the frequency-dependent impedance $Z_L(j\omega)$ of the loads over a broad frequency range. Bandwidth upper bounds are of great help in determining the best achievable bandwidth performance for a given load. Classical Bode-Fano results [1], [2] on the integral of the logarithm of the reflection coefficient can be used for such bounds when there is a single source and load. When there are multiple loads, analyses are often limited to special cases. For example, bandwidth bounds for loads with some specific structures are discussed in [3]–[6], and examples of analyses of multiport systems include [7], [8]. Often, multiple reflection coefficients are defined and analyzed separately using scalar Bode-Fano theory. However, as shown in [9], a physically-meaningful single reflection coefficient can be defined and analyzed when there are N arbitrarily coupled loads driven by N sources ($N > 1$).

In this two-part paper, we present a bandwidth analysis of matched multiport RF systems that builds on bandwidth bounds in [9]. The first part presents the bounds and applies them to systems that can be expressed in closed form. The second part provides proofs of the bounds and applies them to systems whose scattering parameters are expressed numerically. The bounds in [9] apply to loads that are modeled as perfect reflectors as $\omega \to \infty$. We extend these results, and present bounds that apply to loads that are reflectors at any frequency, including $\omega = 0$. We allow the matching network and loads to be non-reciprocal. The network can also be lossy. We permit the number of sources and loads to be unequal.

By applying bandwidth bounds, we demonstrate how the number of sources, loads, and the coupling between loads affect the achievable bandwidth of a matched multiport system. We prove that bandwidth bounds generally scale as N/M, where M is the number of sources and N is the number of loads. This result also holds in the presence of coupling, as long as it is not "too strong". This suggests that unlimited bandwidth is theoretically achievable by simply adding more loads for a fixed number of sources. As is shown, both the loads and the network architecture play an important role in achieving linear-in-N performance of the overall system, for a given M.

We also propose a bandwidth analysis for situations where a portion of the network is constrained to have a certain structure while other portions are unconstrained. This situation occurs in beamforming applications since a beamforming antenna array can be thought of as N loads driven with prescribed amplitude and phase relationships by a single source.

The basic premise of broadband matching is that when a source and load are connected to each other, even if the reflection coefficient is made small at a design frequency $\omega = \omega_d$, it is generally not small for all ω [10]. When there are multiple sources and loads, there is no single reflection coefficient since power sent from source i may, through coupling, return to source $j \neq i$. In [9], a definition of a multiport reflection coefficient that takes this phenomenon into account is used to derive bounds on the ability to match

Ding Nie and Bertrand Hochwald are with the Department of Electrical Engineering, University of Notre Dame, Notre Dame, IN, 46556 USA. E-mail: nding1@nd.edu, bhochwald@nd.edu.

This work was supported, in part, by NSF grants CCF-1403458 and ECCS-1509188.

multiple sources and loads over all ω with a lossless network. We expand this definition to include lossy networks.

Of particular interest is the application to loads that are closely-spaced antennas, such as may be found in multiple-input multiple-output (MIMO) communication systems. The "densification" of portable wireless communication devices, including cellular telephones, with multiple transmitter and receiver chains in close proximity, makes coupling difficult to avoid. Furthermore, there are situations where there are more antennas than RF chains [11]. Our analysis methods quantify the bandwidth attainable in the transmitters of these MIMO systems, where the RF amplifiers are treated as sources and the coupled antennas are the loads. Part II, in particular, shows how realistic antennas are modeled to obtain accurate bandwidth results.

We consider an RF system where M sources drive N loads through an arbitrary passive $(M+N)$-port matching network. The M input ports on the multiport network connect to the sources, and N output ports connect to the loads. No relationship between M and N is assumed. Our goal is to transfer maximum power from sources with known characteristic impedances to loads with known frequency-dependent impedances. The loads are dissipative and potentially non-reciprocal; the network can be lossy and also non-reciprocal. The quality of match between the sources and the loads at a frequency ω is then determined by the power lost either because it is returned to the sources or because it is dissipated in the network. We derive and utilize bounds on this quality metric when an arbitrary passive $(M+N)$-port network is used. Our bounds can readily be calculated from the frequency-dependent S-matrix of the loads.

We do not consider noise in our analysis, and hence our methods apply more to transmitters driving loads than to receivers, where the noise figures of the input amplifiers play an important role. We are interested in the "input bandwidth" of the loads and do not evaluate the ability of the loads to use their input power efficiently.

When the loads are coupled, there is only a nominal association of source i with load i for $i = 1, \ldots, N$ since source i potentially also stimulates load $j \neq i$ if the two loads are coupled. In minimizing the amount of lost power, a matching network between the sources and loads therefore could connect any source with any of the loads, and conversely; examples include decoupling networks [12]–[15], which ensure all power from the sources is delivered to the loads at a design frequency. An effective network prevents reflection by decoupling the loads from each other over as wide a frequency range as possible. Generally, for a given design frequency ω_d, there are frequencies $\omega_1 < \omega_d$ and $\omega_2 > \omega_d$, where the fractional power delivered to the loads falls below some prescribed threshold. The larger $\omega_2 - \omega_1$ is, the larger the bandwidth.

Techniques involving active non-Foster circuits [16], [17] and adaptive matching [18]–[21] are not discussed. Non-Foster circuits such as those used to realize negative capacitance and inductance values can theoretically cancel the reactive Foster behavior in the loads, and achieve an impedance match between the sources and the loads over a wider frequency band than passive networks. Adaptive matching uses tunable capacitors and inductors to match antennas whose impedance is affected by the environment or carrier frequency.

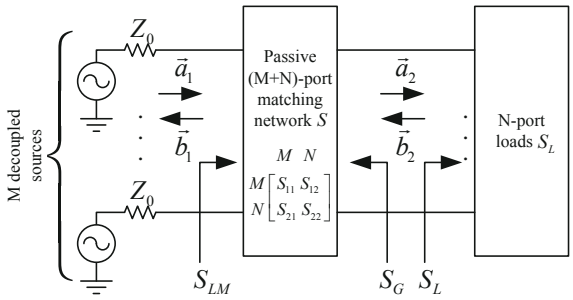

Fig. 1. An RF system where M uncorrelated sources drive N loads having S-matrix S_L through a passive $(M+N)$-port matching network S (the complex-frequency argument s is omitted). We use S_{LM} to denote the S-matrix as seen at the input of the network, and $S_G = S_{22}$ to denote the S-matrix as seen at the output.

The basic model assumptions are given in Section II. The definitions and notations we use are similar to those in [9]. The principal bounds we use are presented in Section III. Details on the mechanics of how to apply these bounds are provided within the subsections of Section III. Analytical applications of the results appear in Section IV, where scaling laws are derived and network architectures are analyzed. Section VI concludes.

The results presented herein assume the loads can be accurately modeled by rational functions of frequency. Since not all loads are necessarily rational, Part II examines how rational functions can be used as approximations for arbitrary loads. We present examples of how to use the bounds in practice. Proofs of all the results are also given.

II. Problem Definition and Notations

A. System description

Figure 1 shows an RF system where N dissipative loads are driven by M decoupled sources with real impedance Z_0, the characteristic impedance of the system. Let $S_L(s)$ be the $N \times N$ S-matrix of the dissipative loads as a function of the complex frequency $s = \sigma + j\omega$, where σ and ω are real. $S_L(s)$ is obtained by extending the S-matrix of the loads $S_L(j\omega)$ as a function of the angular frequency ω to the whole complex plane (WCP). Mathematically, $S_L(s)$ can be thought of as the transfer function between the $N \times 1$ incident and reflected waves $\vec{a}_2 e^{st}$ and $\vec{b}_2 e^{st}$, where t represents time. Therefore, we have $\vec{b}_2(s) = S_L(s)\vec{a}_2(s)$. If the loads are reciprocal then $S_L(s)$ is symmetric. If the loads are coupled, at least one off-diagonal entry of $S_L(s)$ is non-zero. The impedance matrix $Z_L(j\omega)$ of the loads can be obtained by $Z_L(j\omega) = Z_0(I + S_L(j\omega))(I - S_L(j\omega))^{-1}$.

The M sources and N loads are matched by inserting a passive $(M+N)$-port network between them, as indicated in Figure 1. The M input ports of the network are connected to the sources, and the N output ports are connected to the loads. The network is not necessarily lossless or reciprocal, so

we allow standard passive capacitive and inductive elements as well as non-reciprocal ferromagnetic components in its design.

Let $S(s)$ be the $(M+N)\times(M+N)$ S-matrix of the multiport network as a function of s, partitioned as in Figure 1

$$S(s) = \begin{array}{c} \\ M \\ N \end{array} \begin{array}{c} \begin{array}{cc} M & N \end{array} \\ \begin{pmatrix} S_{11}(s) & S_{12}(s) \\ S_{21}(s) & S_{22}(s) \end{pmatrix} \end{array}. \quad (1)$$

Let $S_{LM}(s)$ denote the $M\times M$ S-matrix of the cascade of the network and the loads, and $S_G(s)$ be the $N\times N$ S-matrix seen from the output ports of the network. Since the input to the network is terminated by sources with characteristic impedance Z_0, it follows that $S_G(s)=S_{22}(s)$, and

$$S_{LM}(s)=S_{11}(s)+S_{12}(s)S_L(s)(I-S_G(s)S_L(s))^{-1}S_{21}(s). \quad (2)$$

As in Figure 1, let $M\times 1$ vector $\vec{a}_1(s)$ be the incident wave to the network. Then the reflected wave is $\vec{b}_1(s)=S_{LM}(s)\vec{a}_1(s)$. Since the network is potentially lossy, the incident power may be reflected to the sources (return loss), or dissipated in the network (insertion loss). We now define a measure of performance that includes both of these effects.

B. Power loss ratio

Our measure of performance of a matching network between the sources and loads is given by the fraction of source power that is not transferred to the loads, as a function of frequency. At frequency $s=j\omega$, the total instantaneous power from the M sources is $\|\vec{a}_1(j\omega)\|^2$, and the total instantaneous power delivered to the N loads is $\|\vec{a}_2(j\omega)\|^2-\|\vec{b}_2(j\omega)\|^2\geq 0$. The power lost due to dissipation and reflection is therefore $\|\vec{a}_1(j\omega)\|^2-(\|\vec{a}_2(j\omega)\|^2-\|\vec{b}_2(j\omega)\|^2)$.

Definition 1: The *power loss ratio* at frequency $j\omega$ is the ratio between the expected power loss and the expected total incident power at $j\omega$:

$$r^2(\omega)=\frac{\mathbb{E}\left[\|\vec{a}_1(j\omega)\|^2-(\|\vec{a}_2(j\omega)\|^2-\|\vec{b}_2(j\omega)\|^2)\right]}{\mathbb{E}\,\|\vec{a}_1(j\omega)\|^2}, \quad (3)$$

where the expectation is over the random input signals.

By convention, when we use $r(\omega)$ we mean the positive square root of (3), and by construction, $0\leq r(\omega)\leq 1$ where values close to zero indicate that little source power is being lost and therefore most of it is being delivered to the loads. Values close to one indicate most of the power is lost to dissipation or reflection. We note that $r(\omega)=0$ means that the loads are perfectly matched and decoupled from one another. When the matching network $S(s)$ is lossless, the power loss ratio is equivalent to the power reflection ratio defined in [9]. By considering power dissipation in the network in addition to power reflection by the network, we handle situations that appear favorable because the reflected energy is low, but are actually unfavorable because the network (rather than the load) is dissipating the incident power. This issue is raised in [22].

C. Experimental measurement of $r(\omega)$

Because (3) includes an expectation, we devote a few words to the measurement of $r(\omega)$ in practice. The incident signals from the sources are assumed to have independent random phases and instantaneous powers at each frequency, and the expectation is taken over all such uncorrelated incident signals. Nevertheless, the expectation is unnecessary when $M=1$ since the amplitude and phase of a single source does not affect the power loss ratio. In this case, $1-r^2(\omega)$ is equivalent to the standard transducer power gain [8], [23], and the expectations in the numerator and denominator of (3) may be dropped.

When $M>1$ the expectations play the important role of averaging over all amplitude and phase combinations of the input signals. Its importance can be demonstrated by examining $M=2$, where it is well known that even-mode (in-phase) and odd-mode (out-of-phase) signals can elicit very different reflective responses from a two-port system. Since the sources are uncorrelated, no preference is given to even or odd mode signals, and the expectation eliminates mode dependence by averaging over both of them. Hence, $r(\omega)$ can be thought of as an "average loss" experienced when the loads are stimulated by uncorrelated sources.

The value of $r^2(\omega)$ can be experimentally measured by forming the sample average of the numerator $\|\vec{a}_1(j\omega)\|^2-(\|\vec{a}_2(j\omega)\|^2-\|\vec{b}_2(j\omega)\|^2)$ for a variety of inputs $\vec{a}_1(j\omega)$, and taking the ratio of this average to the sample average of the denominator $\|\vec{a}_1(j\omega)\|^2$. This ratio of averages converges to $r^2(\omega)$ as more measurements are taken with all possible source phase and amplitude combinations.

D. Definition of bandwidth

The network $S(s)$ should be constructed to make $r(\omega)$ as small as possible over a prescribed bandwidth, or make the bandwidth as wide as possible for a prescribed threshold. Usually, bandwidth is measured in the vicinity of a design frequency, which we denote as ω_d. A decoupling network [15] enforces $r(\omega)=0$ at $\omega=\omega_d$. We can define the bandwidth of the combined network and loads using (3).

Definition 2: The *bandwidth* is the frequency range for which $r(\omega)$ is no greater than a threshold $\tau>0$ in the vicinity of a design frequency ω_d:

$$\omega_{\text{BW}}(\tau,\omega_d)=\max_{\substack{\omega_1\leq\omega_d\leq\omega_2\\ r(\omega)\leq\tau,\forall\omega\in[\omega_1,\omega_2]}}\omega_2-\omega_1. \quad (4)$$

Let the elements of $\vec{a}_1(j\omega)$, representing the incident signal from M decoupled sources at frequency $j\omega$, have equal expected square-magnitude over all frequency, and have uniformly distributed random phases in $[0,2\pi)$ that are independent of the amplitudes and each other. Then (3) yields

$$r^2(\omega)=1-\frac{\mathbb{E}\,\text{tr}\{\vec{a}_2^H(j\omega)(I-S_L^H(j\omega)S_L(j\omega))\vec{a}_2(j\omega)\}}{\mathbb{E}\,\text{tr}\{\vec{a}_1^H(j\omega)\vec{a}_1(j\omega)\}}.$$

Because the phases are independent and uniformly distributed, $\mathbb{E}\left[\vec{a}_1(j\omega)\vec{a}_1^H(j\omega)\right]$ is a multiple of the identity matrix. We apply $\vec{a}_2(j\omega)=(I-S_G(j\omega)S_L(j\omega))^{-1}S_{21}(j\omega)\vec{a}_1(j\omega)$ to obtain

$$r^2(\omega)=1-$$

$$\frac{\mathrm{tr}\{S_{21}^H(I-S_GS_L)^{-H}(I-S_L^HS_L)(I-S_GS_L)^{-1}S_{21}\}}{M}, \quad (5)$$

where $\mathrm{tr}(\cdot)$ denotes trace, ^{H} denotes Hermitian transpose; the frequency argument $j\omega$ is omitted on the right-hand side of (5).

When $M > N$, $r^2(\omega) \geq 1 - N/M$ since the matrix inside the trace on the right-hand side of (5) is a rank-N positive semidefinite matrix whose eigenvalues are less than or equal to one. Hence, a certain fraction of the source power is always reflected or absorbed, and letting $\tau < \sqrt{1-N/M}$ in (4) always obtains zero bandwidth. We therefore assume $\sqrt{1-N/M} < \tau < 1$ for $M > N$; for $M \leq N$, we have $0 < \tau < 1$.

Note that "ganging" amplifiers through couplers to attain high output power with a single load appears to be an example where $M > N$. But such ganged sources are correlated since each carries the same signal, possibly differing only in a constant relative phase or amplitude. Since we assume uncorrelated sources, ganged amplifiers (and other correlated sources) should be considered as a single source to apply our results.

Although the incident signals from the sources are assumed to be uncorrelated, the output of the matching network will have correlated components when $M < N$ since any network driving all N loads will necessarily derive its signals from the M sources. As an extreme example, a simple beamformer can be modeled as $M = 1$ source driving $N > 1$ loads in a fixed phase relationship. We consider beamforming in Section V-A.

E. Properties of S-matrices

We briefly summarize some properties of S-matrices since they play an important role. Passive real networks have S-matrices that are real-rational, Hurwitzian, and bounded; this applies, for example, to $S_L(s)$ and $S(s)$. The definitions of these terms can be found in [23]–[25]. We also employ definitions of poles and zeros of rational matrices that are widely used in multivariable control theory [26]. For an arbitrary rational matrix $A(s)$:

- **Poles:** are the roots of the pole polynomial of $A(s)$, where this polynomial is the monic least common multiple of the denominators of all minors of all dimensions of $A(s)$.
- **Zeros:** are the roots of the zero polynomial of $A(s)$, where this polynomial is the monic greatest common divisor of the numerators of all minors of dimension L, and L is the normal rank of $A(s)$. It is assumed that these minors have the pole polynomial as their denominators.

The normal rank of a matrix is its maximum rank among all $s \in \mathbb{C}$; the use of "normal" refers to the rank almost everywhere in the complex plane [24, A.70]. We use LHP to denote the left-half complex plane ($\mathrm{Re}\{s\} < 0$) and RHP to denote the right-half ($\mathrm{Re}\{s\} > 0$). Throughout, we use $p_{L,i}$ and $z_{L,i}$, $i = 1, 2, \ldots$ to represent the poles and zeros over the WCP (whole complex plane) of $S_L(s)$. Since $S_L(s)$ is Hurwitzian, it has no RHP poles.

We assume $I - S_L^T(-s)S_L(s)$ is full normal rank. This is satisfied if the loads are strictly dissipative, so that there is no combination of load signals that is completely reflected for all s. On the other hand, we also assume that there exists an s_0 with $\mathrm{Re}\{s_0\} \geq 0$ such that

$$S_L^T(-s_0)S_L(s_0) = I. \quad (6)$$

In general, s_0 is arbitrary and can be infinite.

When s_0 is purely imaginary $s_0 = j\omega_0$, (6) has the interpretation of modeling the loads as perfect reflectors at frequency ω_0 since $S_L^T(-j\omega) = S_L^H(j\omega)$ and therefore the singular values of $S_L(j\omega_0)$ are all unity. Because $S_L(s)$ is a bounded matrix, (6) is equivalent to $|\det S_L(j\omega_0)| = 1$.

When s_0 has positive real part, the physical interpretation of (6) is elusive but we still use the terminology "perfect reflector" at s_0. Examples of load structures with such an s_0 are given in Section IV-B2.

For any s_0, (6) must also hold if we replace s_0 with $-s_0$. Therefore, without loss of generality, we only consider $\mathrm{Re}\{s_0\} \geq 0$. If there are multiple distinct values of s_0 for which (6) holds then the bounds presented herein apply to each value separately. We therefore consider only a single distinct s_0.

III. Broadband Matching Bounds

We present the principal bounds used in this paper. They are derived in detail in Part II, but knowledge of the derivations is not needed to apply the bounds. A description of how to use these bounds appears in Section III-B. Conditions for achieving equality are presented in Section III-C. The bounds depend on zeros and poles of $S_L(s)$, and techniques to obtain these are discussed in Section III-D and Part II.

A. Principal bounds

Bound 1: For $s_0 = j\omega_0$,

$$\int_0^\infty \frac{(\omega_0-\omega)^{-2}+(\omega_0+\omega)^{-2}}{2}\log\frac{1}{r(\omega)}d\omega \leq \frac{-\pi}{2M}\Big[\sum_i (p_{L,i}-j\omega_0)^{-1}+\sum_i (z_{L,i}+j\omega_0)^{-1}\Big]. \quad (7)$$

Bound 2: For $\mathrm{Re}\{s_0\} > 0$,

$$\int_0^\infty \frac{\mathrm{Re}[(s_0-j\omega)^{-1}+(s_0+j\omega)^{-1}]}{2}\log\frac{1}{r(\omega)}d\omega \leq \frac{-\pi}{2M}\log\left|\det S_L(s_0)\cdot\frac{\prod_i(s_0+z_{L,i})}{\prod_i(s_0-z_{L,i})}\right|. \quad (8)$$

Bound 3: For $s_0 = \infty$,

$$\int_0^\infty \log\frac{1}{r(\omega)}d\omega \leq \frac{-\pi}{2M}\left(\sum_i p_{L,i}+\sum_i z_{L,i}\right). \quad (9)$$

Bound 1 is useful for loads that are modeled as electrically open or short at some frequency $j\omega_0$. For example, some antennas are capacitive relative to ground when they are "electrically small" compared to the signal wavelength. Thus, they are effectively an open circuit at $s_0 = 0$; equivalently $S_L(0) = I$.

Bound 2 applies to loads that are modeled as a mixture of resistive and reactive components [27]. An example of this is given in Section IV-B2.

TABLE I
FORMS OF $f(j\omega)$ AND B IN (10) FOR DIFFERENT LOCATIONS OF s_0, WHERE $p_{L,i}, z_{L,i}$ ARE THE POLES AND ZEROS OF $S_L(s)$.

$s_0 = j\omega_0$	$f(\omega) = \frac{1}{2}[(\omega_0 - \omega)^{-2} + (\omega_0 + \omega)^{-2}]$ $B = \frac{-\pi}{2M}\left[\sum_i (p_{L,i} - j\omega_0)^{-1} + \sum_i (z_{L,i} + j\omega_0)^{-1}\right]$
$\mathrm{Re}\{s_0\} > 0$	$f(\omega) = \frac{1}{2}\mathrm{Re}[(s_0 - j\omega)^{-1} + (s_0 + j\omega)^{-1}]$ $B = \frac{-\pi}{2M}\log\left\lvert\det S_L(s_0)\cdot\frac{\prod_i (s_0+z_{L,i})}{\prod_i (s_0-z_{L,i})}\right\rvert$
$s_0 = \infty$	$f(\omega) = 1$ $B = \frac{-\pi}{2M}\left(\sum_i p_{L,i} + \sum_i z_{L,i}\right)$

Bound 3 applies to loads that are modeled as open or short circuits at infinite frequency. The classical model of a parallel resistive and capacitive load used to demonstrate the Bode-Fano bound falls into this category. A bound similar to (9) is presented in [9]; however, the bound in [9] requires $M = N$ and the matching network to be lossless.

In all three cases, the bounds have the form

$$\int_0^\infty f(\omega)\log\frac{1}{r(\omega)}d\omega \le B, \tag{10}$$

where $f(\omega) \ge 0$. The form of $f(\omega)$ depends on the location of s_0, and the computation of B depends also on the poles and zeros of $S_L(s)$. Because $0 \le r(\omega) \le 1$, we have $\log(1/r(\omega)) \ge 0$. Hence, $f(\omega)\log(1/r(\omega)) \ge 0$ for any ω. Clearly, B must be positive as well. We use (10) to generically indicate any of (7)–(9). The number of sources appears as M in the denominators of all three bounds. The forms of $f(\omega)$ and B are summarized in Table I.

B. How to use bounds

Suppose that we wish to assess the achievable bandwidth $[\omega_1, \omega_2]$ of a set of loads, where $\omega_1 < \omega_2$. Our measure of achievability is that for some threshold $\tau > 0$, the overall system should obey $r(\omega) \le \tau$ for $\omega \in [\omega_1, \omega_2]$. Hence the combined multiport network and loads reflects (or absorbs) no more than τ within the passband. We assume that $S_L(s)$ is available to us (we have more to say about this in Section III-D) and we would like to know $\omega_{\mathrm{BW}}(\tau, \omega_d)$ defined in (4).

Suppose the loads obey $S_L^T(0)S_L(0) = I$ so that Bound 1 (first row of Table I) with $\omega_0 = 0$ applies to any passive network used for these loads. Let the right-hand side of (7) be denoted $B_1 > 0$, which depends only on $S_L(s)$. Then

$$\begin{aligned} B_1 \ge \int_0^\infty \omega^{-2}\log\frac{1}{r(\omega)}d\omega &\ge \log\frac{1}{\tau}\int_{\omega_1}^{\omega_2}\omega^{-2}\,d\omega \\ &= \log\frac{1}{\tau}\left(\frac{1}{\omega_1} - \frac{1}{\omega_2}\right). \end{aligned}$$

The first inequality applies to any network, while the second inequality applies to a network with the desired passband characteristics. Hence,

$$\frac{1}{\omega_1} - \frac{1}{\omega_2} \le \frac{B_1}{\log(1/\tau)}. \tag{11}$$

Clearly, this inequality imposes a constraint on (ω_1, ω_2) pairs.

Bounds 2 and 3 can be applied in a similar fashion. If $S_L^H(\infty)S_L(\infty) = I$, (9) gives

$$\omega_2 - \omega_1 \le \frac{B_3}{\log(1/\tau)}, \tag{12}$$

where B_3 is the right-hand side of (9). This gives us a direct bound on the bandwidth $\omega_{\mathrm{BW}}(\tau, \omega_d)$ achievable for all ω_d. Equations (11) and (12) are complementary in that both can be in force simultaneously.

We now discuss conditions under which these bounds can be achieved.

C. Conditions for equality

We distinguish between conditions for equality in (7)–(9) and conditions for equality in (11), (12). The former apply to any passive real network and the latter apply to networks with particular passband characteristics. Bounds (7)–(9) have a common set of conditions for achieving equality:

1) $S_{21}(s)S_{21}^T(-s) + S_G(s)S_G^T(-s) = I$ for all s
2) The $M \times M$ matrix
$$S_{21}^H(I - S_G S_L)^{-H}(I - S_L^H S_L)(I - S_G S_L)^{-1}S_{21} \tag{13}$$
has equal singular values for all $s = j\omega$
3) $I - S_L(s_0)S_G(s_0)$ is non-singular
4) $S_L^T(-s) - S_G(s)$ has no zeros in the RHP

where s_0 is defined in (6). These four conditions correspond to four possible impediments to achieving the bounds. Meeting all the conditions is sufficient to attain equality in the bounds, but Conditions 1, 2 and 4 are also necessary. The $N \times N$ matrix $S_G(s)$ (see Figure 1) plays a prominent role in these conditions and can be readily measured or modeled by connecting pairs of output ports of the matching network to a network analyzer while terminating its remaining ports with characteristic impedances.

These conditions have physical interpretations. Condition 1 is satisfied for lossless networks since we are guaranteed that $S_{21}(s)S_{21}^T(-s) + S_{22}(s)S_{22}^T(-s) = I$ for all s because $S(s)$ is a para-unitary matrix, and $S_G(s) = S_{22}(s)$.

Condition 2 requires the singular values of (13) to be equal for all $s = j\omega$. When this is satisfied, the total dissipated power at the loads depends only on the total incident power $\|\vec{a}_1(j\omega)\|^2$, and not the "direction" of $\vec{a}_1(j\omega)$.

Condition 3 is a "non-degenerate" condition that we illustrate with an example: Suppose the loads are capacitive to ground, and hence are reflective with $S_L(\infty) = -I$. If the output impedance of the matching network is also capacitive, then $S_G(\infty) = -I$ and Condition 3 is violated. Hence, in this example, a matching network that wants to achieve high bandwidth should avoid capacitive output impedance. It turns out that Condition 3 is superfluous in Bound 2 because $S_L(s)$ and $S_G(s)$ are bounded matrices; hence $S_L(s)S_G(s)$ is also bounded and $I - S_L(s_0)S_G(s_0)$ is always non-singular for $\mathrm{Re}\{s_0\} > 0$ [24, 7.22]. Additional details on Condition 3 can be found in [9].

Condition 4 is a "minimum-phase" condition since the RHP zeros of $S_L^T(-s) - S_G(s)$ are the same as the RHP zeros of $S_{GM}(s)$, which involves a "Darlington equivalent" network

representation of the loads [28], [29] as described in Part II. However, knowledge of the Darlington equivalent network is not needed to check this condition. We have more to say about network architectures that cannot meet this condition in Section IV-C.

Assuming Conditions 1–4 are met by the matching network, we obtain equality in (11), (12) if the network also achieves the ideal response $r(\omega) = \tau$ for $\omega \in [\omega_1, \omega_2]$ and $r(\omega) = 1$ elsewhere. Any network such that $r(\omega) < 1$ for $\omega \notin [\omega_1, \omega_2]$ sustains a non-negative "shaping loss" which is the difference between the integral over all ω of the left-hand sides of (7)–(9) versus the integral over $[\omega_1, \omega_2]$:

$$\text{shaping loss} = \int_0^\infty f(\omega) \log \frac{1}{r(\omega)} d\omega - \int_{\omega_1}^{\omega_2} f(\omega) \log \frac{1}{r(\omega)} d\omega. \qquad (14)$$

For a network whose shaping loss is positive, some performance is lost in the band of interest because either $\omega_2 - \omega_1$ could potentially be made larger, or τ could be made smaller, by redesigning the network to have larger $r(\omega)$ for $\omega \notin [\omega_1, \omega_2]$. We provide an example of the shaping loss computation in Part II, Section III-A.

D. How to obtain $S_L(s)$ and its poles and zeros

If analytical circuit models for the loads are known, $S_L(s)$ is uniquely determined by the standard Laplace transform representations of the model impedance or admittance matrix and using the formula $S_L(s) = (Z_L(s) + Z_0 I)^{-1}(Z_L(s) - Z_0 I)$. Examples of this are presented in Section IV-B.

Absent an analytical model, numerical methods that model the $S_L(s)$ of the loads are needed to extract its poles and zeros. The modeling methods are discussed and illustrated by example in Part II.

IV. Bandwidth Analysis

The bounds yield a variety of conclusions when they are applied to various system configurations. We first examine decoupled loads in Section IV-A and then coupled loads in IV-B. We then identify network architectures that can achieve the bounds in Section IV-C.

A. Decoupled loads

Let $S_L(s) = S_l(s)I$ where $S_l(s)$ is a scalar and I is an $N \times N$ identity matrix. Thus, there are N decoupled identical loads. Let $S_l(s)$ satisfy (6) for some s_0, and let B_l be computed using Table I applied to $S_l(s)$ for $M = 1$. Then $S_L(s)$ satisfies (6) at the same s_0, and has poles and zeros at the same locations as $S_l(s)$, each with multiplicity N. It follows from Table I that the bound for N loads is N times the bound for a single load. We have proven the following theorem.

Theorem 1: For N identical decoupled loads driven by M sources

$$\int_0^\infty f(\omega) \log \frac{1}{r(\omega)} d\omega \le \frac{N}{M} B_l. \qquad (15)$$

If $N = M$, (15) is simply B_l. This is not surprising because we have assumed the sources and loads are decoupled and therefore we are essentially examining N identical isolated systems, each with bound B_l. However, (15) scales linearly with N for a fixed M. This formula suggests that N identical decoupled loads can achieve N times the bandwidth of one load as long as the matching network is designed properly.

Matching network architectures can be thought of in terms of their ability to achieve linear-in-N bandwidth behavior when used with a set of loads with linear-in-N behavior. In Section IV-C we show that certain network architectures provably have linear-in-N behavior, while others do not. As shown in the next section, this linear-in-N behavior extends to coupled loads under some conditions.

B. Circulantly-coupled loads

Loads with circulant $S_L(s)$ are especially easy to manipulate mathematically because, while the eigenvalues of $S_L(s)$ depend on s, its eigenvectors do not. This makes computing $p_{L,i}$ and $z_{L,i}$ straightforward. Load structures that lead to symmetric circulant $S_L(s)$ are identical, and the coupling between load i and neighbor j depends on $\min\{|i-j|, N-|i-j|\}$.

Two identical loads automatically have circulant symmetry, as long as they have reciprocal coupling. Three or more loads can be placed in a circular or spherical arrangement to yield circulant $S_L(s)$.

1) Loads exemplifying Bound 1: Figure 2(a) illustrates N circulantly-coupled loads. The loads consist of an N-port inductive network with impedance matrix sZ_l and an N-port series LC network with impedance matrix $\frac{s^2/\omega_0^2+1}{2s} Z_{lc}$ resonating at $j\omega_0$. These networks are connected in parallel to each other, and terminated by isolated characteristic impedances Z_0. The parallel N-port networks are shown in Figure 2(b,c); the inductive network has each port grounded through L_0 and every pair of ports i and j is connected through L_ℓ, where $\ell = \min\{|i-j|, N-|i-j|\}$ is the "distance" between ports i and j. The series LC network has each port grounded through L_0' and C_0', and every pair of ports i and j is connected through L_ℓ' and C_ℓ', where $\sqrt{L_0'C_0'} = \sqrt{L_\ell'C_\ell'} = 1/\omega_0^2$. The $N \times N$ matrices Z_l and Z_{lc} are circulant symmetric.

Since circulant matrices have eigenvectors that are columns of a discrete Fourier transform (DFT) matrix, we obtain the following eigenvalue decompositions:

$$Z_l = W \Lambda_l W^H, \quad Z_{lc} = W \Lambda_{lc} W^H,$$

where

$$W = \frac{1}{\sqrt{N}} \begin{bmatrix} 1 & 1 & \cdots & 1 \\ 1 & e^{-\frac{j2\pi}{N}} & \cdots & e^{-\frac{j2\pi(N-1)}{N}} \\ \vdots & \vdots & \ddots & \vdots \\ 1 & e^{-\frac{j2\pi(N-1)}{N}} & \cdots & e^{-\frac{j2\pi(N-1)^2}{N}} \end{bmatrix} \qquad (16)$$

is the $N \times N$ unitary DFT matrix, and Λ_l and Λ_{lc} are real positive diagonal matrices representing the eigenvalues of Z_l and Z_{lc}, respectively.

The impedance matrix of the loads is

$$Z_L(s) = \left(\frac{1}{s} Z_l^{-1} + \frac{2s}{s^2/\omega_0^2 + 1} Z_{lc}^{-1} + \frac{1}{Z_0} I \right)^{-1}.$$

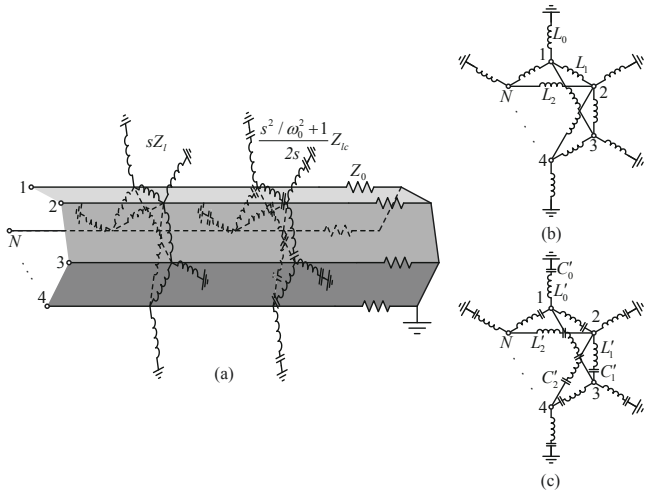

Fig. 2. (a) N circulantly-coupled loads consisting of an inductive network and an LC network in parallel, terminated in a set of characteristic impedances Z_0. The inductive and the LC portions of the network are shown in (b,c), and have impedance matrices sZ_l and $\frac{s^2/\omega_0^2+1}{2s}Z_{lc}$, respectively. The loads are coupled to ground through L_0 and series L_0' and C_0', and every load pair is coupled through L_ℓ and series L_ℓ' and C_ℓ', where ℓ is the "distance" between the pair.

Then $S_L(s)$ can be obtained from $S_L(s) = (Z_L(s) + Z_0 I)^{-1}(Z_L(s) - Z_0 I)$, which is

$$S_L(s) = W \frac{-Z_0[(2\Lambda_{lc}^{-1}\omega_0^2+\Lambda_l^{-1})s^2+\Lambda_l^{-1}\omega_0^2]}{2s^3+Z_0(2\Lambda_{lc}^{-1}\omega_0^2+\Lambda_l^{-1})s^2+2\omega_0^2 s+Z_0\Lambda_l^{-1}\omega_0^2} W^H. \tag{17}$$

Note, we write $(\cdot)^{-1}$ as $\frac{1}{(\cdot)}$ when we take inverses of diagonal matrices. Because $S_L(s)$ is a circulant matrix, only its eigenvalues depend on s and the poles and zeros of $S_L(s)$ are therefore the poles and zeros of the individual eigenvalues.

All N loads present short circuits to ground at $s_0 = 0$ and $j\omega_0$, where the loads become perfect reflectors. Hence, $S_L(0) = S_L(j\omega_0) = -I$, and (6) is satisfied. We can then obtain two distinct bounds by applying Bound 1 for $s_0 = 0$ and $j\omega_0$. Using $p_{L,i}, z_{L,i}$ calculated from (17), Bound 1 yields

$$\int_0^\infty \omega^{-2} \log \frac{1}{r(\omega)} d\omega \le \frac{-\pi}{2M} \sum_i \frac{-2\lambda_{l,i}}{Z_0} = \frac{\pi \cdot \mathrm{tr} Z_l}{MZ_0}, \tag{18a}$$

$$\int_0^\infty \frac{(\omega_0-\omega)^{-2}+(\omega_0+\omega)^{-2}}{2} \log \frac{1}{r(\omega)} d\omega \le \frac{-\pi}{2M} \sum_i \frac{-2\lambda_{lc,i}}{Z_0\omega_0^2} = \frac{2\pi \cdot \mathrm{tr} Z_{lc}}{MZ_0\omega_0^2}. \tag{18b}$$

The ith diagonal element of Z_l represents the inductance relative to ground of port i of the inductive network in Figure 2(b), measured with the remaining ports open. Because Z_l is circulant its diagonal elements are all equal. Hence $(1/N)\mathrm{tr} Z_l = L_{\mathrm{eq},N}$, where $L_{\mathrm{eq},N}$ is the inductance of any port relative to ground. A similar conclusion holds for the LC network in Figure 2(c). Let the equivalent series LC branch of any port relative to ground have inductance $L'_{\mathrm{eq},N}$ and capacitance $C'_{\mathrm{eq},N}$, where $L'_{\mathrm{eq},N}C'_{\mathrm{eq},N} = 1/\omega_0^2$. Then $(1/N)\mathrm{tr} Z_{lc} = \omega_0^2 L'_{\mathrm{eq},N} + 1/C'_{\mathrm{eq},N}$. We can rewrite (18) as

$$\int_0^\infty \omega^{-2} \log \frac{1}{r(\omega)} d\omega \le \frac{N\pi L_{\mathrm{eq},N}}{MZ_0}, \tag{19a}$$

$$\int_0^\infty \frac{(\omega_0-\omega)^{-2}+(\omega_0+\omega)^{-2}}{2} \log \frac{1}{r(\omega)} d\omega \le \frac{N\pi}{MZ_0}\left(L'_{\mathrm{eq},N} + \frac{1}{\omega_0^2 C'_{\mathrm{eq},N}}\right), \tag{19b}$$

Let $L_{\mathrm{eq},N}$, $L'_{\mathrm{eq},N}$ and $C'_{\mathrm{eq},N}$ approach respective limits L_{eq}, L'_{eq} and C'_{eq} as $N \to \infty$. We have proven the following theorem.

Theorem 2: The linear-in-N behavior shown in Theorem 1 for decoupled loads extends to circulantly-coupled loads provided $L_{\mathrm{eq}} > 0$ and $L'_{\mathrm{eq}} > 0$ (or $C'_{\mathrm{eq}} < \infty$).

The conditions $L_{\mathrm{eq}} > 0$ and $L'_{\mathrm{eq}} > 0$ (or $C'_{\mathrm{eq}} < \infty$) are equivalent to ensuring that the inductance (or capacitance) of any port relative to ground does not go to zero (or infinity) as $N \to \infty$, and hence there are not "too many" parallel paths to ground from any port. This is equivalent to imposing a condition that the coupling between loads not be "too strong".

For a given N and M, the bounds in (19) for Figure 2 increase as inductive and capacitive coupling components are removed, since $L_{\mathrm{eq},N}$ increases and approaches L_0 as all cross-inductive elements are removed; similarly $L'_{\mathrm{eq},N}$ increases to L_0' and $C'_{\mathrm{eq},N}$ decreases to C_0' because $L_{\mathrm{eq},N}$, $L'_{\mathrm{eq},N}$ and $C'_{\mathrm{eq},N}$ are obtained as L_0, L_0' and C_0' in parallel with the remaining parts of the networks.

However, we cannot conclude that coupling always has a negative effect on bandwidth. In fact, Part II of this paper shows that coupling between dipole antennas has a non-monotonic effect on the bandwidth bound. This dichotomy in behavior between the model in Figure 2 and the dipoles in Part II is not contradictory because there is no requirement that dipoles should be modeled by fixed L_0, L_0', and C_0' as the coupling between them changes.

2) Loads exemplifying Bound 2: Figure 3 illustrates N resistors Z_0 terminated with two parallel N-port networks: one is resistive with $N \times N$ circulant impedance matrix Z_r, and the other is capacitive with $N \times N$ circulant impedance matrix $\frac{1}{s}Z_c$. The impedance matrix of the loads $Z_L(s)$ is

$$Z_L(s) = Z_0 I + (Z_r^{-1} + sZ_c^{-1})^{-1}.$$

Let Λ_r and Λ_c be the eigenvalue matrices of Z_r and Z_c. Then $S_L(s)$ is

$$S_L(s) = W \frac{\Lambda_r\Lambda_c}{2Z_0\Lambda_r s + 2Z_0\Lambda_c + \Lambda_r\Lambda_c} W^H \tag{20}$$

where W is given in (16).

We note that

$$I - S_L^T(-s)S_L(s) = W \frac{-4Z_0^2\Lambda_r^2 s^2 + 4Z_0(Z_0 I + \Lambda_r)\Lambda_c^2}{-4Z_0^2\Lambda_r^2 s^2 + (2Z_0 I + \Lambda_r)^2\Lambda_c^2} W^H.$$

Let the component values satisfy $\frac{\Lambda_c\sqrt{Z_0(Z_0I+\Lambda_r)}}{Z_0\Lambda_r} = \sigma_0 I$ for some $\sigma_0 > 0$. Then (6) is satisfied for $s_0 = \sigma_0$. We substitute $\Lambda_c = \frac{Z_0\Lambda_r\sigma_0}{\sqrt{Z_0(Z_0I+\Lambda_r)}}$ into (20), and apply (8) to yield

$$\int_0^\infty \frac{\sigma_0}{\sigma_0^2+\omega^2} \log \frac{1}{r(\omega)} d\omega$$

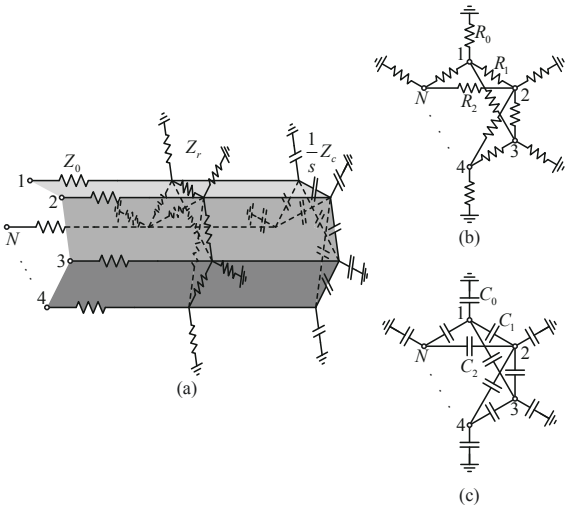

Fig. 3. (a) N circulantly-coupled loads consisting of N resistors Z_0 in series with a parallel resistive network Z_r and a parallel capacitive network $\frac{1}{s}Z_c$. The resistive and the capacitive portions of the network are shown in (b,c), and have respective impedance matrices Z_r and $\frac{1}{s}Z_c$. The loads are coupled to ground through R_0 and C_0, and every load pair is coupled through R_ℓ and C_ℓ, where ℓ is the "distance" between the pair.

$$\leq \frac{-\pi}{2M}\log\det\frac{\Lambda_r}{2Z_0+\Lambda_r+2\sqrt{Z_0(Z_0+\Lambda_r)}}$$
$$=\frac{\pi}{2M}\sum_{i=1}^{N}\log\frac{2Z_0+\lambda_{r,i}+2\sqrt{Z_0(Z_0+\lambda_{r,i})}}{\lambda_{r,i}}, \qquad (21)$$

where $\lambda_{r,i}$ are the diagonal elements of Λ_r. The linear-in-N behavior of these loads depends on $\lambda_{r,1},\ldots,\lambda_{r,N}$; we do not pursue this analysis any further here.

C. Ability of network architecture to achieve bounds

Matching network architectures that cannot achieve equality in the bounds should be identified whenever possible and removed from consideration in large-bandwidth applications. The following theorem shows how $S_G(s)$ defined in Figure 1 can be compared with $S_L(s)$ to identify such networks. We thereby make Condition 4 in Section III-C more physically tangible.

Theorem 3: For matching networks satisfying Condition 3, if $S_G(s)$ has an eigenvector in common with $S_L(s)$, and the associated eigenvalue $\lambda_G(s)$ satisfies $|\lambda_G(j\omega)|=1$ for all ω, then Condition 4 cannot be satisfied and therefore the bounds cannot be achieved.

Proof: See the Appendix. ∎

Theorem 3 can be applied to the example of decoupled loads in Section IV-A. We assume $1\leq M<N$ and Condition 3 is satisfied. Since $S_L(s)=S_l(s)I$, any vector is an eigenvector of $S_L(s)$. Theorem 3 then implies that any $S_G(s)$ that has $|\lambda_G(j\omega)|=1$ cannot achieve equality in (15).

For example, networks where $S_G(s)$ is a real symmetric matrix cannot achieve equality. This follows because even if the network is lossless and Condition 1 is satisfied, implying that $S_{21}(s)S_{21}^T(-s)+S_G(s)S_G^T(-s)=I$ for all s, then because $S_{21}(s)$ is an $N\times M$ matrix and $S_G(s)$ is an $N\times N$ matrix, $S_G(s)$ has at least $N-M$ unit singular values. Since the moduli of the eigenvalues of a real symmetric matrix are equal to its singular values, at least one eigenvalue satisfies $|\lambda_G(j\omega)|=1$. We conclude that reciprocal broadband splitters or couplers that yield real symmetric $S_G(s)$ cannot be used to achieve equality in (15) when $M<N$ and the loads are decoupled. We see an example of this in the next section.

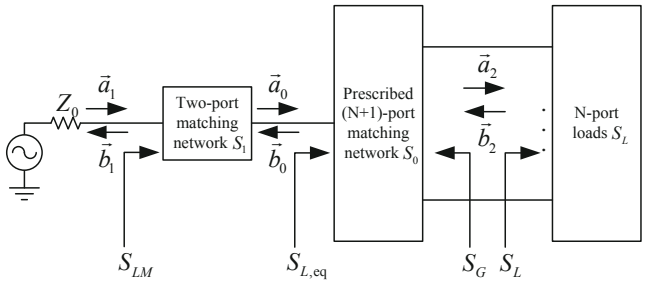

Fig. 4. An RF system where one source drives N loads having S-matrix S_L through a constrained matching network consisting of a prescribed $(N+1)$-port network S_0 and an arbitrary network S_1 (the complex-frequency argument s is omitted). We use $S_{L,\text{eq}}$ to denote the S-parameter seen from the input of S_0.

V. One Source and Multiple Loads

We probe the special case of one source more deeply with some examples in this section. We analyze constrained networks in Section V-A. One source with many loads is examined in Sections V-B and V-C, leading to a class of non-reciprocal networks called "determinant" networks.

A. Constrained matching network

Let a portion of the network be constrained or prescribed to have a particular structure. For example, the constrained portion might include ideal circulators or power splitters. The prescribed portion and loads then together constitute an "equivalent load" and the achievable bandwidth is determined by the characteristics of this load.

Figure 4 illustrates an example of such a structure for $M=1$, where a prescribed $(N+1)$-port network is combined with the loads and forms an equivalent one-port load. Let the S-matrix of the prescribed network be

$$S_0(s)=\begin{array}{c}\\1\\N\end{array}\begin{array}{c}\begin{array}{cc}1 & N\end{array}\\\begin{pmatrix}S_{0,11}(s) & S_{0,12}(s)\\ S_{0,21}(s) & S_{0,22}(s)\end{pmatrix}\end{array}.$$

Then the S-parameter of the equivalent load is

$$S_{L,\text{eq}}(s)=S_{0,11}(s)+S_{0,12}(s)S_L(s)(I-S_{0,22}(s)S_L(s))^{-1}S_{0,21}(s). \qquad (22)$$

The remaining unspecified portion of the network $S_1(s)$ is connected to the input port of $S_{L,\text{eq}}(s)$, and we may ask what bandwidth is attainable by $S_1(s)$.

Generally, we cannot apply the bounds directly to $S_{L,\text{eq}}(s)$. Unlike $S_L(s)$ where power is either dissipated or reflected by the loads, power in $S_{L,\text{eq}}(s)$ can also be absorbed by the constrained portion of the network when $S_0(s)$ is lossy. Let

$\eta(\omega)$ denote the ratio between the power dissipated by $S_L(s)$ and the power delivered to $S_{L,\text{eq}}(s)$, defined as

$$\eta(\omega) = \frac{\|\vec{a}_2(j\omega)\|^2 - \|\vec{b}_2(j\omega)\|^2}{\|a_0(j\omega)\|^2 - \|b_0(j\omega)\|^2},$$

where $(\vec{a}_2(j\omega),\ \vec{b}_2(j\omega))$ and $(a_0(j\omega),\ b_0(j\omega))$ are the (incident, reflected) signals from $S_L(s)$ and $S_{L,\text{eq}}(s)$, respectively. Then $0 \le \eta(\omega) \le 1$ and

$$\eta(\omega) = \frac{S_{0,21}^H (I - S_{0,22}S_L)^{-H}(I - S_L^H S_L)(I - S_{0,22}S_L)^{-1}S_{0,21}}{1 - S_{L,\text{eq}}^H S_{L,\text{eq}}}, \tag{23}$$

which depends only on the prescribed network and the loads.

We assume $S_{L,\text{eq}}(s)$ satisfies (6) for some s_0; this does not require $S_L(s)$ to satisfy (6) for the same s_0. Then (10) becomes the following bound.

Theorem 4: For loads matched by a constrained network,

$$\int_0^\infty f(\omega) \log \sqrt{\frac{\eta(\omega)}{r^2(\omega) + \eta(\omega) - 1}} d\omega \le B_{\text{eq}} \tag{24}$$

where B_{eq} is the right-hand side of (10) applied to $S_{L,\text{eq}}(s)$.

Proof: Using Figure 4, we define

$$r_{\text{eq}}^2(\omega) = 1 - \frac{\|a_0(j\omega)\|^2 - \|b_0(j\omega)\|^2}{\|a_1(j\omega)\|^2}$$

as the ratio between power not delivered to $S_{L,\text{eq}}(s)$ and the incident power from the source. Then it follows that

$$\begin{aligned} r^2(\omega) &= 1 - \frac{\|\vec{a}_2(j\omega)\|^2 - \|\vec{b}_2(j\omega)\|^2}{\|a_1(j\omega)\|^2} \\ &= 1 - \frac{\|a_0(j\omega)\|^2 - \|b_0(j\omega)\|^2}{\|a_1(j\omega)\|^2} \cdot \frac{\|\vec{a}_2(j\omega)\|^2 - \|\vec{b}_2(j\omega)\|^2}{\|a_0(j\omega)\|^2 - \|b_0(j\omega)\|^2} \\ &= 1 - (1 - r_{\text{eq}}^2(\omega)) \cdot \eta(\omega). \end{aligned}$$

Equivalently, we have $r_{\text{eq}}(\omega) = \sqrt{\frac{r^2(\omega)+\eta(\omega)-1}{\eta(\omega)}}$.

We apply (10) to the equivalent load $S_{L,\text{eq}}(s)$. The result is an inequality on $r_{\text{eq}}(\omega)$:

$$\int_0^\infty f(\omega) \log \frac{1}{r_{\text{eq}}(\omega)} d\omega \le B_{\text{eq}},$$

where B_{eq} is the right-hand side of (10) applied to $S_{L,\text{eq}}(s)$. Replacing $r_{\text{eq}}(\omega)$ with $\sqrt{\frac{r^2(\omega)+\eta(\omega)-1}{\eta(\omega)}}$ gives us (24). ∎

We use beamforming as an example application. Let the desired amplitude and phase relationship of the antennas be denoted by the $N \times 1$ unit real-rational vector $\vec{v}(s)$ for $s = j\omega$. Then

$$S_0(s) = \begin{bmatrix} 0 & \vec{v}^T(s) \\ \vec{v}(s) & 0 \end{bmatrix} \tag{25}$$

denotes the S-matrix of a reciprocal one-to-N power divider that constrains the incident signal $\vec{a}_2(j\omega)$ to be aligned with $\vec{v}(j\omega)$. We are not concerned with the so-called gain-bandwidth product of a phased array [30] which measures its ability to maintain far-field gain across a range of frequencies.

Theorem 5: Let the beamforming vector $\vec{v}(s)$ be a real constant unit eigenvector of $S_L(s)$. Then

$$\int_0^\infty f(\omega) \log \frac{1}{r(\omega)} d\omega \le B_{\text{eq}}, \tag{26}$$

where B_{eq} is calculated using $S_{L,\text{eq}}(s) = \vec{v}^T(s) S_L(s) \vec{v}(s)$.

Proof: We substitute (25) into (22) and (23), where $S_{0,11} = 0$, $S_{0,12} = \vec{v}^T(s)$, $S_{0,21} = \vec{v}(s)$ and $S_{0,22} = 0$. Then (22) yields

$$S_{L,\text{eq}}(s) = \vec{v}^T(s) S_L(s) \vec{v}(s),$$

and (23) yields

$$\eta(\omega) = \frac{\vec{v}^H(I - S_L^H S_L)\vec{v}}{1 - S_{L,\text{eq}}^H S_{L,\text{eq}}} = \frac{\vec{v}^H\vec{v} - \vec{v}^H S_L^H S_L \vec{v}}{1 - \vec{v}^H S_L^H \vec{v}^* \vec{v}^T S_L \vec{v}}.$$

Because $\vec{v}(s)$ is a real unit eigenvector of $S_L(s)$, it is readily verified that $\eta(\omega) = 1$. The result then follows by applying Theorem 4. ∎

Section III-B in Part II of this paper provides an example where B_{eq} in (26) varies with the choice of $\vec{v}(s)$.

We note that $\eta(\omega) = 1$ is obtained for any lossless $S_0(s)$, in which case (26) also applies. When $\eta(\omega) = 1$ and $S_L(s)$ satisfies (6) for some s_0, then $S_{L,\text{eq}}(s)$ also satisfies (6) for the same s_0; the converse is not true.

Compared with (10), (26) is smaller for $N > 1$. To see this more explicitly, let the loads be decoupled as in Section IV-A, whence $S_L(s) = S_l(s)I$. Then any real constant unit vector $\vec{v}(s)$ satisfies $\eta(\omega) = 1$, and the equivalent load satisfies $S_{L,\text{eq}}(s) = S_l(s)$. Then Theorem 5 yields

$$\int_0^\infty f(\omega) \log \frac{1}{r(\omega)} d\omega \le B_l, \tag{27}$$

where B_l is the right-hand side of (10) applied to $S_l(s)$ for $M = 1$, Clearly, $B_l < NB_l$, which is the bound obtained in (15) for $M = 1$. We conclude that linear-in-N behavior is not generally achieved for the beamforming structure (25). This conclusion is consistent with Theorem 3.

B. Decoupled loads

Section IV-C says that full bandwidth cannot be achieved when reciprocal broadband splitters are used to drive $N > 1$ loads when $M = 1$. We instead consider a matching network consisting of non-reciprocal couplers in Figure 5(a) where an $(N+1)$-port network comprising $N-1$ circulators as the constrained part of the network is displayed. The resulting $(N+1) \times (N+1)$ S-matrix is

$$S_0(s) = \begin{bmatrix} 0 & 0 & \cdots & 0 & 1 \\ 1 & 0 & \cdots & 0 & 0 \\ 0 & 1 & 0 & \cdots & 0 \\ \vdots & 0 & \ddots & \ddots & \vdots \\ 0 & \cdots & 0 & 1 & 0 \end{bmatrix}.$$

The lower right $N \times N$ block of this matrix, which corresponds to $S_G(s)$, has N zero eigenvalues and therefore does not satisfy the conditions of Theorem 3. Let $S_{L,\text{eq}}(s)$ be the S-matrix of the equivalent one-port load seen at the input of the circulators. Because the circulators are lossless,

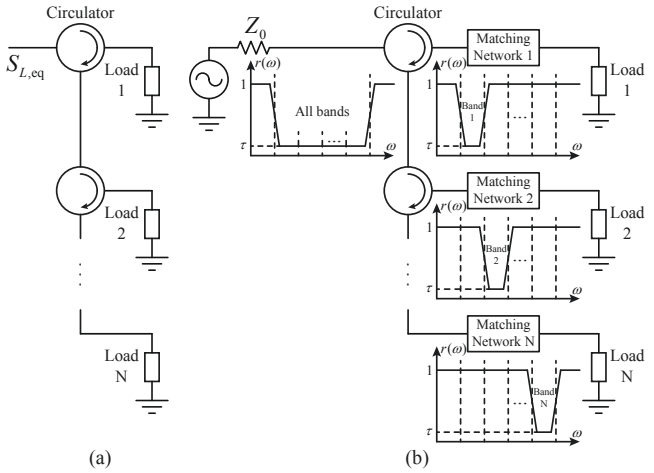

Fig. 5. (a) $N-1$ circulators are used to match N decoupled loads to $M=1$ source, and achieve linear-in-N behavior. We use $S_{L,\text{eq}}(s)$ to denote the S-parameter of the equivalent one-port load seen at the input of the circulators. (b) N decoupled loads are driven by $M=1$ source through N two-port networks and $N-1$ broadband circulators. Each of the two-ports matches $1/N$ of the total bandwidth; network i passes band i and reflects the remaining portions. The circulators combine all N passbands and achieve a total bandwidth N times of the bandwidth of each two-port network.

$\eta(\omega)=1$ in this constrained network. It is readily calculated that $S_{L,\text{eq}}(s)=[S_l(s)]^N$, which has poles and zeros at the same locations as $S_l(s)$, each with multiplicity N. Therefore, according to (10), the bandwidth achievable with this equivalent $S_{L,\text{eq}}(s)$ is N times that achievable by $S_l(s)$. Hence, linear-in-N network behavior for N decoupled loads can be achieved by ideal circulators.

This circulator-based network architecture presents "multiple opportunities" for the energy that is reflected from any one load to be forwarded to the next for another attempt at transmission. We are ignoring the insertion losses associated with cascading circulators in such an arrangement.

Figure 5(b) has a structure similar to Figure 5(a) but matches $1/N$ of the total bandwidth in an orderly fashion. The first network passes the lowest portion of the band and reflects all the remaining portions, which are passed to the next circulator which matches the next portion, and so on. This structure resembles a channelizer [31] in the sense that there are multiple output ports where each port contains a portion of the total bandwidth. Although we have drawn these networks as having near-ideal flat frequency responses, this aspect is not crucial. An explicit example of this type of network for a pair of dipoles is presented in Section III-A in Part II.

C. Circulantly-coupled loads: Determinant networks

The previous section gave a circulator-based architecture for achieving linear-in-N bandwidth for N uncoupled loads. We now show how to handle circulantly coupled loads such as examined in Section IV-B, by demonstrating a network architecture that converts the multiport system with S-matrix $S_L(s)$ into a single-port system with S-parameter $S_{L,\text{eq}}(s)=\det S_L(s)$. Since $\det S_L(s)$ has the same poles and zeros as $S_L(s)$ if $S_L(s)$ has no cancelling poles and zeros, $S_{L,\text{eq}}(s)$ has the same bound as $S_L(s)$. We denote any network that converts $S_L(s)$ into $\det S_L(s)$ a "determinant network". Determinant networks are linear-in-N.

Let W be defined as in (16) and have columns $\vec{w}_1,\dots\vec{w}_N$. Define $W_1=[\vec{w}_2\ \vec{w}_3\ \cdots\ \vec{w}_N\ \vec{0}]$ and the $(N+1)\times(N+1)$ matrix

$$S_0(s)=\begin{bmatrix} 0 & \vec{w}_N^H \\ \vec{w}_1 & W_1W^H \end{bmatrix}. \tag{28}$$

Notice that W_1 is missing the column $\vec{w}_1$. Then $S_0(s)$ is constant and lossless. The following theorem says that it is also a determinant network.

Theorem 6: Let the network described by (28) have its N outputs connected to any circulantly-coupled set of loads with S-matrix $S_L(s)$. Then its input has equivalent S-parameter $S_{L,\text{eq}}(s)=\det S_L(s)$.

Proof: We let $L=W^HW_1$ and use the eigenvalue decomposition $S_L(s)=W\Lambda(s)W^H$ where $\Lambda(s)=\text{diag}(\lambda_1(s),\dots,\lambda_N(s))$ is a diagonal matrix of eigenvalues. Then (22) yields

$$\begin{aligned} S_{L,\text{eq}}(s) &= \vec{w}_N^H S_L(s)(I-W_1W^HS_L(s))^{-1}\vec{w}_1 \\ &= \vec{w}_N^H W\Lambda(s)W^H(I-WL\Lambda(s)W^H)^{-1}\vec{w}_1 \\ &= \begin{bmatrix} 0 & \cdots & 0 & \lambda_N(s) \end{bmatrix}(I-L\Lambda(s))^{-1} \\ &\quad\times\begin{bmatrix} 1 & 0 & \cdots & 0 \end{bmatrix}^T, \end{aligned}$$

where

$$I-L\Lambda(s)=\begin{bmatrix} 1 & 0 & \cdots & & 0 \\ -\lambda_1(s) & 1 & 0 & \cdots & 0 \\ 0 & -\lambda_2(s) & 1 & & 0 \\ \vdots & & \ddots & \ddots & \vdots \\ 0 & \cdots & 0 & -\lambda_{N-1}(s) & 1 \end{bmatrix}.$$

It follows that $S_{L,\text{eq}}(s)$ is $\lambda_N(s)$ times the $(N,1)$ entry of $(I-L\Lambda(s))^{-1}$. This gives $S_{L,\text{eq}}(s)=\prod_{n=1}^N\lambda_n(s)$. ■

An intuitive explanation of the operation of the network is as follows. The network (28) orients the power from the source along the first eigenvector $\vec{w}_1$. Energy is then reflected by the loads with amplitude $\lambda_1(s)$ along $\vec{w}_1$, at which point the determinant network reflects it entirely back to the loads, but with orientation $\vec{w}_2$. This is reflected by the loads with amplitude $\lambda_2(s)$ which is returned by the network to the loads reoriented along $\vec{w}_3$, and so on. The last eigenvector $\vec{w}_N$ reflected by the loads is returned to the source. The result is an overall S-parameter with value $\prod_{n=1}^N\lambda_n(s)$, which is the determinant of $S_L(s)$. This description also explains why a determinant network is not unique.

For example, for $N=2$,

$$S_0(s)=\begin{bmatrix} 0 & \frac{1}{\sqrt{2}} & -\frac{1}{\sqrt{2}} \\ \frac{1}{\sqrt{2}} & \frac{1}{2} & \frac{1}{2} \\ \frac{1}{\sqrt{2}} & -\frac{1}{2} & -\frac{1}{2} \end{bmatrix}. \tag{29}$$

As can by seen by this S-matrix, the network works by first exciting the even mode of the coupled loads. Any reflected power, which is also in an even mode, is then converted into an odd-mode excitation.

One possible realization of (29) is given in Figure 6, which utilizes an ideal transformer and gyrator. A gyrator with resistance Z_0 is transparent to forward propagating waves but

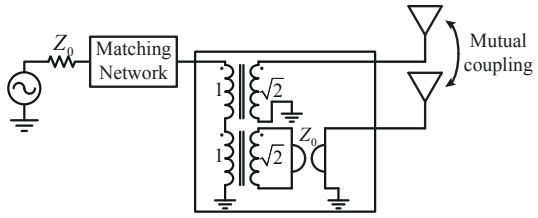

Fig. 6. Realization of the network (29) that includes a transformer and non-reciprocal gyrator connected to two coupled antennas.

behaves as a π phase shift for reverse waves. The network in Figure 6 converts the wave incident on the transformer primary into an even-mode excitation for the loads on its secondaries. Any power reflected by the loads, which is also in an even mode, is converted into an odd mode by the gyrator. The secondaries of the transformer acts like an open circuit to this odd-mode signal. The signal is therefore reflected by the transformer back to the loads as an odd-mode excitation. Finally, any odd-mode excitation reflected by the antennas is then converted by the gyrator into an even-mode signal and passed by the transformer back to the source.

The network in Figure 6 can achieve the bound in (10) for a single source and two identical loads that are reciprocally coupled. This network would also work well for the decoupled loads in Section IV-A since decoupled loads are trivially reciprocal. Note that the circulator structure proposed in Figure 5 is a determinant network when the loads are decoupled but is otherwise not. Hence, the network in Figure 6 generalizes the networks in Figure 5 for $N = 2$.

VI. Conclusions

We have presented bandwidth analyses for multiport RF systems using bandwidth upper bounds that apply to an arbitrary number of sources and loads, and allows arbitrary coupling between the loads. Conditions for achieving equality in the bounds were discussed. We demonstrated that the bandwidth bounds scale generally as N/M for M sources and N loads. We focused on loads whose scattering matrices can be expressed analytically with rational functions.

In Part II of this paper, we apply the upper bounds to realistic loads whose scattering parameters are expressed numerically and therefore need to be approximated by rational functions. The accuracy needed of such approximations is analyzed. Some of the effects of coupling are examined in detail, and complete derivations of the bounds are also provided.

Appendix
Proof of Theorem 3

Let $\vec{v}(s)$ be the eigenvector of $S_L(s)$ and $S_G(s)$ associated with eigenvalues $\lambda_L(s)$ and $\lambda_G(s)$. Because $S_L(s), S_G(s)$ are bounded matrices, $\lambda_L(s), \lambda_G(s)$ are bounded functions. Since $|\lambda_G(j\omega)| = 1$, $\lambda_G(s)$ is an all-pass function with all poles in the LHP and zeros in the RHP. Moreover, because $I - S_L^T(-s)S_L(s)$ is full normal rank and $S_L(s)$ satisfies (6), $\lambda_L(s)$ is non-constant and satisfies $\lambda_L(-s_0)\lambda_L(s_0) = 1$ where s_0 is defined in (6). Thus, $|\lambda_L(s)| < 1$ for $\mathrm{Re}\{s\} > 0$, $|\lambda_G(s)| \geq 1$ for $\mathrm{Re}\{s\} < 0$ and $|\lambda_G(s)| \leq 1$ for $\mathrm{Re}\{s\} > 0$; the equalities holds if $\lambda_G(s)$ is a constant.

We start by showing $\vec{v}^H(j\omega)S_G(j\omega) = \lambda_G(j\omega)\vec{v}^H(j\omega)$. Since $\lambda_G(j\omega)$ and $\vec{v}(j\omega)$ are an eigenvalue-eigenvector pair of $S_G(j\omega)$,

$$\vec{v}^H(j\omega)(S_G(j\omega) - \lambda_G(j\omega)I)\vec{v}(j\omega) = 0.$$

Suppose $\vec{u}^H(j\omega) = \vec{v}^H(j\omega)(S_G(j\omega) - \lambda_G(j\omega)I) \neq 0$, then $\vec{u}(j\omega) \perp \vec{v}(j\omega)$, and

$$\begin{aligned}\|\vec{v}^H(j\omega)S_G(j\omega)\| &= \|\lambda_G(j\omega)\vec{v}^H(j\omega) + \vec{u}^H(j\omega)\| \\ &> \|\lambda_G(j\omega)\vec{v}^H(j\omega)\| = \|\vec{v}^H(j\omega)\|.\end{aligned}$$

But because $S_G(s)$ is bounded, all singular values of $S_G(j\omega)$ are no greater than one. This contradicts with the inequality above. Hence, $\vec{u}^H(j\omega) = 0$, and we have $\vec{v}^H(j\omega)S_G(j\omega) = \lambda_G(j\omega)\vec{v}^H(j\omega)$.

Let $\vec{v}'(s)$ be the extension of $\vec{v}^*(j\omega)$ to the WCP. We then show that Condition 4 cannot be achieved when Condition 3 is satisfied. We need to show $\vec{v}'^T(s)(S_L^T(-s) - S_G(s)) = (\lambda_L(-s) - \lambda_G(s))\vec{v}'^T(s) = 0$ for some s in the RHP. It suffices to show $\lambda_L(-s) - \lambda_G(s) = 0$.

Since $|\lambda_L(-s)| < 1$ and $|\lambda_G(s)| \geq 1$ for $\mathrm{Re}\{s\} < 0$, all zeros of $\lambda_L(-s) - \lambda_G(s) = 0$ must locate in $\mathrm{Re}\{s\} \geq 0$. Both $\lambda_L(s)$ and $\lambda_G(s)$ are rational functions, so we let their degrees be n_1 and n_2, respectively. Since all the poles of $\lambda_L(s)$ and $\lambda_G(s)$ are in the LHP, the poles of $\lambda_L(-s)$ and $\lambda_G(s)$ do not coincide. Hence $\lambda_L(-s) - \lambda_G(s)$ has degree $n_1 + n_2$. Moreover, $|\lambda_L(j\omega)| = 1$ has at most n_1 solutions; this is because $1 - \lambda_L(-s)\lambda_L(s)$ has degree at most $2n_1$, and any zeros of $1 - \lambda_L(-s)\lambda_L(s)$ on the imaginary axis have multiplicity at least two. Since $|\lambda_G(j\omega)| = 1$ for all ω, $\lambda_L(-s) - \lambda_G(s)$ has at most n_1 zeros on the imaginary axis. This leaves at least n_2 zeros in the RHP, and we have proven the theorem when $n_2 \geq 1$.

When $n_2 = 0$, we prove by contradiction. Suppose all n_1 zeros of $\lambda_L(-s) - \lambda_G(s)$ are on the imaginary axis. Then the zeros of $1 - \lambda_L(-s)\lambda_L(s)$ are at the same locations as the zeros of $\lambda_L(-s) - \lambda_G(s)$. Because we assume $\lambda_L(-s_0)\lambda_L(s_0) = 1$ for some s_0, s_0 must be one of the zeros of $\lambda_L(-s) - \lambda_G(s)$. Thus, we have $\lambda_G(s_0) = \lambda_L(-s_0)$, and $1 - \lambda_G(s_0)\lambda_L(s_0) = 0$. This contradicts Condition 3. Hence, $\lambda_L(-s) - \lambda_G(s)$ has zeros in the RHP when $n_2 = 0$. Thus, Condition 4 is not met, and since this condition is necessary for achieving the bounds, the bounds cannot be met with equality. ■

References

[1] H. W. Bode, *Network Analysis and Feedback Amplifier Design,* New York, NY: Van Nostrand, 1945.

[2] R. M. Fano, "Theoretical limitations on the broadband matching of arbitrary impedances," *Journal of the Franklin Institute,* 249(1) pp. 57–83, and 249(2), pp. 139–154, 1950.

[3] Z.-M. Wang and W.-K. Chen, "Broad-band matching of multiport networks," *IEEE Trans. Circ. Sys.*, vol. 31, no. 9, pp. 788–796, Sep. 1984.

[4] S. Nordebo and M. Gustafsson, "Multichannel broadband Fano theory for arbitrary lossless antennas with applications in DOA estimation," *2005 IEEE International Conference on Acoustics, Speech, and Signal Processing,* pp. 969–972, March 2005.

[5] P. S. Taluja and B. L. Hughes, "Bandwidth limitations and broadband matching for coupled multi-antenna systems," *Proc. 2011 IEEE Global Telecomm. Conf. (GLOBECOM),* Houston, TX, Dec. 2011.

[6] P. S. Taluja and B. L. Hughes, "Diversity limits of compact broadband multi-antenna systems," *IEEE J. Sel. Area Comm.,* vol. 31, no. 2, pp. 326–337, Feb. 2013.

[7] B. K. Lau, J. B. Andersen, G. Kristensson and A. F. Molisch, "Impact of matching network on bandwidth of compact antenna arrays," *IEEE Trans. Ant. Prop.*, vol. 54, no. 11, pp. 3225–3238, Nov. 2006.

[8] J. C. Allen, J. Rockway and D. Arceo, "Wideband multi-port matching phase I: single-feed multiport antennas," Tech. Rep. 1972, SSC San Diego, Sep. 2008. Download available at www.dtic.mil/dtic/tr/fulltext/u2/a487970.pdf.

[9] D. Nie and B. M. Hochwald, "Broadband matching bounds for coupled loads," *IEEE Trans. Circ. Sys. I: Regular Papers,* vol. 62, no. 4, pp. 995–1004, April 2015.

[10] D. M. Pozar, *Microwave Engineering,* 4th ed., Hoboken, NJ: Wiley, 2011.

[11] A. Alkhateeb, O. El Ayach, G. Leus, R. W. Heath, "Channel estimation and hybrid precoding for millimeter wave cellular systems," *IEEE J. Sel. Topics Signal Process.,* vol. 8, no. 5, pp. 831–846, Oct. 2014.

[12] J. W. Wallace and M. A. Jensen, "Mutual coupling in MIMO wireless systems: a rigorous network theory analysis," *IEEE Trans. on Wireless Comm.,* vol. 3, no. 4, pp. 1317–1325, July 2004.

[13] J. Weber, C. Volmer, K. Blau, R. Stephan and M. A. Hein, "Miniaturized antenna arrays using decoupling networks with realistic elements," *IEEE Trans. Micro. Thy. Tech.*, vol. 54, no. 6, pp. 2733–2740, June 2006.

[14] A. Krewski and W. L. Schroeder, "N-port DL-MIMO antenna system realization using systematically designed mode matching and mode decomposition network," *42nd Eur. Micro. Conf. (EuMC),* pp. 156–159, Oct. 2012.

[15] D. Nie, B. M. Hochwald and E. Stauffer, "Systematic design of large-scale multiport decoupling networks," *IEEE Trans. Circ. Sys. I: Regular Papers,* vol. 61, no. 7, pp. 2172–2181, July 2014.

[16] J. T. Aberle, "Two-port representation of an antenna with application to non-Foster matching networks," *IEEE Trans. Ant. Prop.*, vol. 56, no. 5, pp. 1218–1222, May 2008.

[17] S. E. Sussman-Fort and R. M. Rudish, "Non-Foster impedance matching of electrically-small antennas," *IEEE Trans. Ant. Prop.*, vol. 57, no. 8, pp. 2230–2241, Aug. 2009.

[18] J. de Mingo, A. Valdovinos, A. Crespo, D. Navarro and P. Garcia, "An RF electronically controlled impedance tuning network design and its application to an antenna input impedance automatic matching system," *IEEE Trans. Micro. Thy. Tech.,* vol. 52, no. 2, pp. 489–497, Feb. 2004.

[19] A. van Bezooijen, M. A. de Jongh, F. van Straten, R. Mahmoudi, A. H. M. van Roermund, "Adaptive impedance-matching techniques for controlling L networks," *IEEE Trans. Circ. Sys. I: Regular Papers,* vol. 57, no. 2, pp. 495–505, Feb. 2010.

[20] Q. Gu and A. S. Morris, "A new method for matching network adaptive control," *IEEE Trans. Micro. Thy. Tech.,* vol. 61, no. 1, pp. 587–595, Jan. 2013.

[21] R. Mohammadkhani and J. S. Thompson, "Adaptive uncoupled termination for coupled arrays in MIMO systems," *IEEE Trans. Ant. Prop.*, vol. 61, no. 8, pp. 4284–4295, Aug. 2013.

[22] J. C. Allen, D. Arceo and P. Hansen,"Optimal lossy matching by Pareto fronts," *IEEE Trans. Circ. Sys. II: Express Briefs,* vol. 55, no. 6, pp. 497–501, June 2008.

[23] R. W. Newcomb, *Linear Multiport Synthesis,* New York, NY: McGraw-Hill, 1966.

[24] V. Belevitch, *Classical Network Theory,* San Francisco, CA: Holden-Day, 1968.

[25] M. R. Wohlers, *Lumped and Distributed Passive Networks: A Generalized and Advanced Viewpoint,* New York, NY: Academic Press, 1969.

[26] S. Skogestad and I. Postlethwaite, *Multivariable Feedback Control: Analysis and Design,* 2nd ed., Hoboken, NJ: Wiley, 2005.

[27] D. C. Youla, "A new theory of broad-band matching," *IEEE Trans. Circ. Thy.,* vol. 11, no. 1, pp. 30–50, March 1964.

[28] S. Darlington, "Synthesis of reactance 4-poles," *Journal of Mathematics and Physics,* vol. XVIII, pp. 275–353, Sep. 1939.

[29] R. Douglas, J. Helton, "The precise theoretical limits of causal Darlington synthesis," *IEEE Trans. Circ. Thy.,* vol. 20, no. 3, pp. 327–327, May 1973.

[30] R. J. Mailloux, *Phased Array Antenna Handbook,* 2nd ed., Norwood, MA: Artech House, 2005.

[31] C. J. Galbraith, R. D. White, L. Cheng, K. Grosh and G. M. Rebeiz, "Cochlea-based RF channelizing filters," *IEEE Trans. Circ. Sys. I: Regular Papers,* vol. 55, no. 4, pp. 969–979, May 2008.